

An experimental method to calculate the on-axis dose in small field for stereotactic radiotherapy

Talal Abdul Hadi^{1,2}, Rezart Belshi¹, Gauthier Bouilhol¹, Abdulhamid Chaikh³, Pascal François⁴

¹Department of Radiation Oncology and Medical Physics, Hospital René Huguenin, Curie Institute, Saint-Cloud, France

²School of GEET, Toulouse III University, Toulouse, France

³Department of Radiation Oncology and Medical Physics, Grenoble-Alpes University Hospital, Grenoble, France

⁴Department of Medical physics, CHU Jean-Bernard, Poitiers, France

Received January 22, 2016; Revised September 21, 2016; Accepted October 10, 2016; Published Online October 30, 2016

Original Article

Abstract

Purpose: The use of small fields in advanced radiotherapy techniques has increased, in particular in stereotactic treatments. However, measuring on-axis dose in such fields is challenging. In this study, we developed an analytic model to accurately estimate the on-axis dose in small fields. **Methods:** Our study was carried out using 6 MV photon beams from four linear accelerators and with three dosimeters placed in a water tank: EBT3 Gafchromic films, a 31016 PinPoint ionization chamber and a 60017 E diode. The out-of-field leakage factor defined as the ratio of the central axis dose to the off-axis dose was modeled. On-axis doses estimated from out-of-field measurements were compared with the measured ones. **Results:** The experimental validation of the present method was performed for square and rectangular fields with sizes ranging from $0.5 \times 0.5 \text{ cm}^2$ to $10 \times 10 \text{ cm}^2$. We found the leakage factor exhibits an exponential decrease independent of the accelerator. This behavior can be integrated in the model to estimate the on-axis dose with an agreement better than 2% compared to EBT3 film measurements at a 10 cm depth and an 8 cm cross-plane off-axis distance. **Conclusion:** We have developed an analytic model to estimate the on-axis dose in small fields based on the out-of-field leakage measurement. This model can be used to validate dose and output factor measurements.

Keywords: Stereotactic radiotherapy, Small field, Dose measurement, Leakage factor

1. Introduction

The main objective of radiotherapy is to obtain the highest probability of tumor control or cure with the lowest amount of morbidity and toxicity to normal tissues. Currently, numerous different irradiation techniques, such as radiosurgery (SRS) and volumetric modulated arc therapy (VMAT), use photon fields smaller than $2 \times 2 \text{ cm}^2$.¹ Such complex techniques allow better dose conformity using a multi-leaf collimator (MLC), a μ -MLC or stereotactic cones to shape the beam.²⁻³ Due to a high complexity, a specific quality assurance (QA) process is required to compare the calculated dose given by the treatment planning system (TPS) with the measured delivered dose. However, accurate dose determination is critical and challenging for small photon fields because of the lack of electron equilibrium and the perturbations introduced by the detector itself.⁴⁻⁵ These perturbations can be due to the

density and size of the sensitive volume, atomic properties and the presence of extra camera components.⁶⁻⁸ The studies showed there is no linearity between fields sizes defined by the collimator and the 50% isodose.⁹⁻¹⁰ However, the energy spectrum of the secondary electrons slightly changes with field sizes.¹¹ This will result in dose under- and/or overestimations depending on the off-axis distance.¹²⁻¹⁴ There is a wide range of recommendations and protocols for small field measurements.¹⁵⁻²⁰ Several dosimeters are currently available to monitor the dose and improve the quality of patient care in small field radiation therapy such as Gafchromic films, ionization chambers or semiconductor diodes. Gafchromic films give a good estimate of small field output factors but their preparation is a tedious process. In this study, we propose a method to accurately estimate the on-axis dose based on off-axis

Corresponding author: Talal Abdul Hadi; Department of Radiation Oncology and Medical Physics, Hospital René Huguenin, Curie Institute, Saint-Cloud, France.

Cite this article as: Abdul-Hadi T, Belshi R, Bouilhol G, Chaikh A, François P. An experimental method to calculate the on-axis dose in small field for stereotactic radiotherapy. *Int J Cancer Ther Oncol*. 2016; 4(4):443. DOI: 10.14319/ijcto.44.3

measurements. We experimentally validated the method for small beams from four linear accelerators: NovalisTx, TrueBeam, Clinac600, and Primus. The experiments were carried out using a water tank and the dose measurements were carried out using Gafchromic films, ionization chamber and diode.

2. Methods and Materials

2.1. Dose modeling

In general, the delivered dose (D) by an accelerator, in a phantom, in isocentric conditions can be calculated using the following formalism²¹:

$$D(z, c, 0) = \dot{D}(z_R, c_R) \times MU \times O_R(z_R, c) \times TPR(z, c) \quad (1)$$

where \dot{D} is the dose rate, M the number of monitor units, O_R the output ratio measured in full scatter conditions (large phantom) and T is the tissue-phantom ratio. The parameters z, c are the measurement depth and the square field size, respectively, and z_R, c_R are the corresponding parameters in reference conditions. To take into account off-axis points, Equation 1 becomes:

$$D(z, c, r) = \dot{D}(z_R, c_R, r_R) \times MU \times O_R(z_R, c, r_R) \times TPR(z, c, r_R) \times OAR(z, c, r) \quad (2)$$

where O is the off-axis ratio, r is the off-axis distance and r_R is the off-axis distance in reference conditions.

Let K_{leak} be the ratio of the central axis dose D_{axis} to the off-axis dose $D_{off-axis}$:

$$K_{leak}(z, c, r) = \frac{D_{axis}}{D_{off-axis}} = \frac{D(z, c, 0)}{D(z, c, r)} \quad (3)$$

and using Equation 2:

$$K_{leak}(z, c, r) = \frac{OAR(z, c, 0)}{OAR(z, c, r)} = \frac{1}{OAR(z, c, r)} \quad (4)$$

In this paper, we propose to model K_{leak} as a function of the field size to estimate the D_{axis} as:

$$D_{axis} = D_{off-axis} \times K_{leak}(z, c, r) \quad (5)$$

In this study, K_{leak} was measured for 6 MV beams from 4 accelerators. To validate our method we compared the dose calculated with Equation 5 with the measured doses using EBT3 films in the same conditions. Figure 1 shows the principle of the method. Measurements were

performed at the isocenter at a depth of 10 cm and at 8 cm off-axis distance for square and rectangular fields. Measurements were carried out for different numbers of MU and five times to evaluate the repeatability and reproducibility. The difference between measured and calculated doses was calculated as:

$$\Delta dose = \frac{D_{calculated} - D_{measured}}{D_{measured}} \times 100 \quad (6)$$

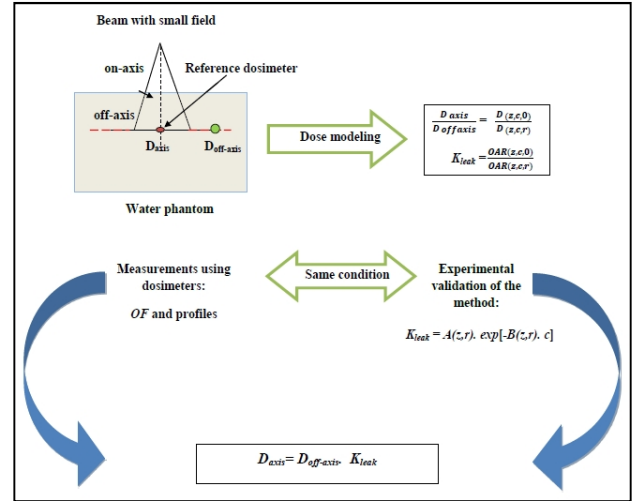


Figure 1: Principle of the method.

2.2. Detectors and measurements

The measurements were performed with EBT3™ Gafchromic films, an ionization chamber and a diode. EBT3 films are water proof and near tissue-equivalent.²² EBT3 films have a symmetric structure and the active layer is placed between two transparent polyester substrates with 100 μm. The polyester has a surface containing microscopic silica particles, which create a large enough gap between the surface and the active layer, eliminating the interference pattern of Newton rings. The advantage is the possibility to irradiate and scan the film on both sides. Film were scanned using an Epson Expression 10 000 XL scanner and the FilmQAPro® software.

The ion chamber was a 3D PinPoint (PTW Freiburg, type 31016). The chamber has a cylindrical air cavity of 0.016 cm³, featuring a central aluminum electrode. The sensitive volume is 2.9 mm in diameter and 2.9 mm in length. The diode was an E Diode (PTW Freiburg, type 60017) with a nominal sensitive volume of 0.03 mm³ with circular of 1 mm² and a thickness of 30 μm. The 3D Pinpoint and the E diode were connected to a PTW electrometer.

The experimentation was carried out using a water tank (WELHOFER IBA Dosimetry Blue 3D) of 67 x 65 x 56 cm³. The phantom was connected to the OminPro-Accept 6.6 system which allows automatically moving the detectors inside the phantom.

The detectors above-mentioned are widely used to measure the physical characteristics of small fields. This includes the percent depth dose curves, cross beam profiles and output ratios.

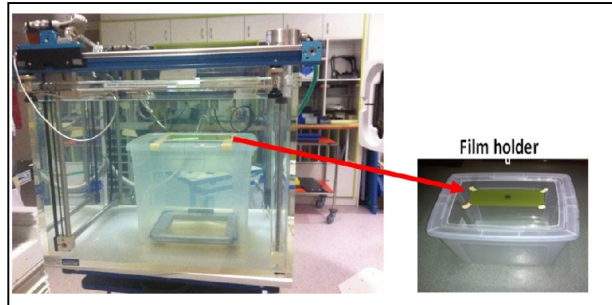


Figure 2: EBT3 film and detector experimental set-up using the water tank.

2.3. Experimental set-up

Table 1: Output factors for the NovalisTx 6 MV beam measured in the water phantom at a 10 cm depth and a 100 cm SDD.

Field size [cm ²]	3DPinPoint chamber	E diode	EBT3 film	Diff % diode vs. film	Diff % film vs. chamber
0.5×0.5	0.376	0.505	0.481	+4.9	-27.9
0.8×0.8	0.571	0.653	0.632	+3.3	-10.6
1×1	0.645	0.694	0.679	+2.2	-5.2
1.5×1.5	0.736	0.755	0.751	+0.5	-2
2×2	0.779	0.780	0.778	0.2	0.1
3×3	0.82	0.824	0.825	0.1	0.06
4×4	0.858	0.855	0.859	0.3	0.03
8×8	0.959	0.959	0.960	0.08	0.07
10×10	1.000	1.000	1.000	-	-

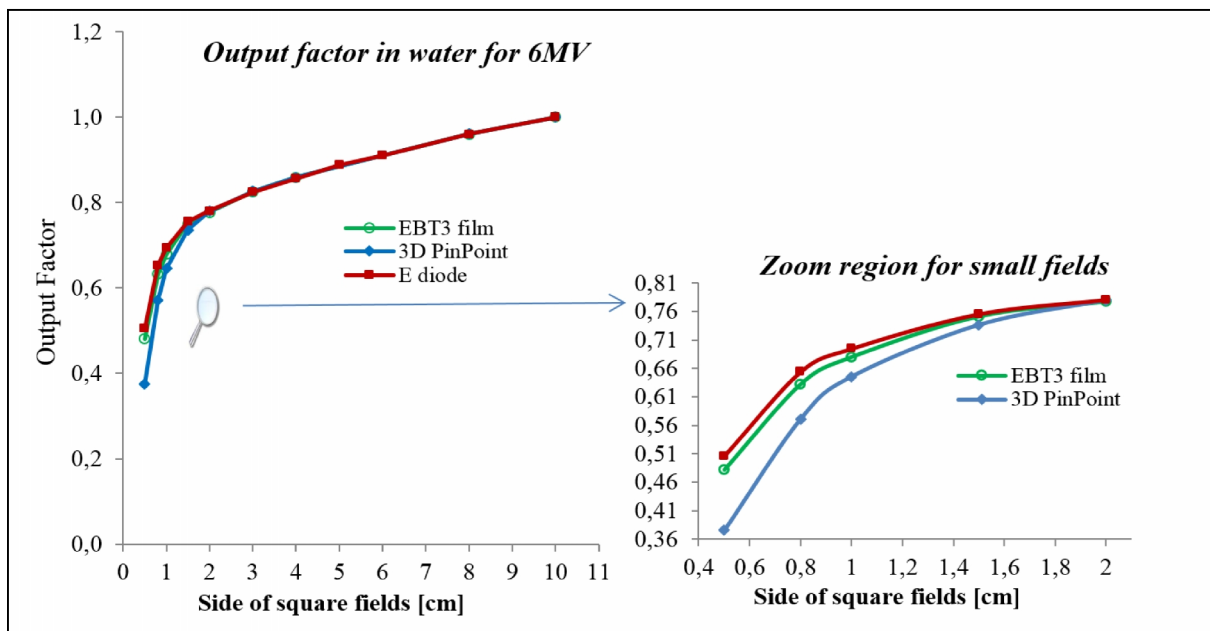


Figure 3: Left panel shows output factors measured in water phantom using EBT3 films, a 3D PinPoint chamber and an E diode for the NovalisTx 6 MV beam. Right panel shows a zoom for field sizes from $0.5 \times 0.5 \text{ cm}^2$ to $2 \times 2 \text{ cm}^2$.

3. Results

3.1. Output Factor

Figure 3 shows output factors measured using EBT3 films, the 3D PinPoint chamber and the E diode. The measurements were carried out using the 6 MV beam from the NovalisTx system, at a 10 cm depth and a 100 cm SDD, for fields varying from $0.5 \times 0.5 \text{ cm}^2$ to $10 \times 10 \text{ cm}^2$. It can be seen that the output factors measured with the 3D PinPoint chamber were lower than the output factors measured with EBT3 films for small fields smaller than $2 \times 2 \text{ cm}^2$. Differences ranged from 0.4% for the $2 \times 2 \text{ cm}^2$ field to 27.9% for the $0.5 \times 0.5 \text{ cm}^2$ field. We also observed an over-response of the E Diode (2% for the $1 \times 1 \text{ cm}^2$ field). Table 1 shows the measured values.

Table 2: Values of leakage parameters, A and B, at 8 cm off-axis distance and a 10 cm depth. The delivered dose was 400 MU using 6 MV beams.

Machine	A	B [cm^{-1}]
Jaws		
Novalis Tx	435.13	0.316
TrueBeam	460.74	0.324
Clinac600	445.26	0.316
Jaws+MLC		
Novalis Tx	260.59	0.254
Primus	230.19	0.239

3.2. Profile measurements

Figure 4 shows the profiles using 6 MV beam from NovalisTx. Figure 5 shows a zoom for the region outside the field. The profiles were measured at 10 cm of depth using EBT3 films, the 3D PinPoint ion chamber and the E diode. The profiles are presented in absolute doses to illustrate the influence of detector size on dose measurements. It can be seen in Figures 4 and 5 a huge effect of the detector size on the measured dose, especially for the smallest field size ($0.5 \times 0.5 \text{ cm}^2$). In the peak position, the difference between films and chamber is close to 30%. Similarly, to the output factor measurements, the profiles were underestimated using an ion chamber and slightly overestimated with the diode compared with the films. However, it is interesting

to note that the detectors measured similar profiles within 2% outside the field for off-axis distances larger than 7 cm. This means that the detectors measured the same scattered dose outside the field with high precision and there is no impact of the detector size on dose measurements in this area. According to this result, a cross-plane 8 cm off-axis distance was chosen to measure the out-of-field dose and then to calculate the on-axis dose.

3.3. Leakage factor (K_{leak})

Figure 6 shows the relationship between K_{leak} and the field size at a 10 cm depth and a 8 cm off-axis distance for 6 MV beams. The measurements were carried out with the 3D PinPoint chamber and EBT3 films. It can be seen in Figure 6 that the relationship between K_{leak} and the field size can be modeled by:

$$K_{\text{leak}}(z, c, r) = A(z, r) \times e^{-B(z, r) \times c} \quad (7)$$

where $A(z, r)$ and $B(z, r)$ are the specific leakage constants. A is without unity and B in cm^{-1} . The size of the field defined as: $c = \sqrt{x \cdot y}$.

EBT3 films were used for field sizes from $0.5 \times 0.5 \text{ cm}^2$ to $3 \times 3 \text{ cm}^2$ and the 3D PinPoint chamber was used for field sizes from $3 \times 3 \text{ cm}^2$ to $10 \times 10 \text{ cm}^2$. Table 2 presents the values of A and B in equation (7) in the same condition for Figure 6. The delivered dose was 400 MU using jaws alone or jaws with MLC. It can be seen that A and B values are independent of the machine for the 6 MV energy.

3.4. Experimental validation of the method for D_{axis}

The measurements showed a good repeatability and reproducibility with deviations lower than 2%. Table 3 shows the dose measured with EBT3 films and calculated using equations 5. The delivered doses were 200, 400 and 800 MU. It can be seen that the difference between measured and calculated doses was less than 2%. We also used the model to calculate the dose in rectangular fields and we observed a dose deviation of 1.1% for a $0.5 \times 1 \text{ cm}^2$ and 0.93 % for a $1 \times 2 \text{ cm}^2$.

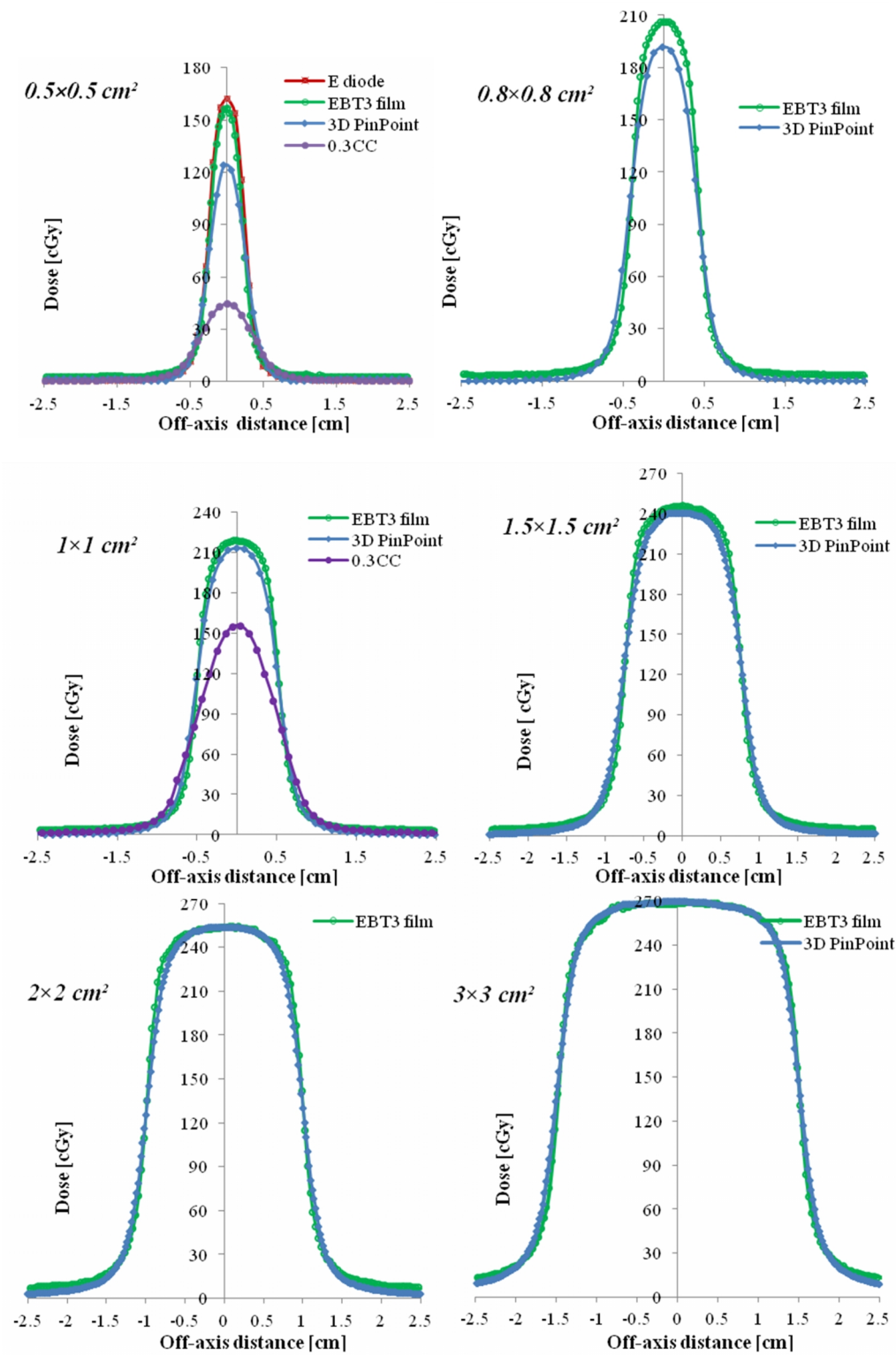


Figure 4: Profiles for the NovalisTx 6MV beam.

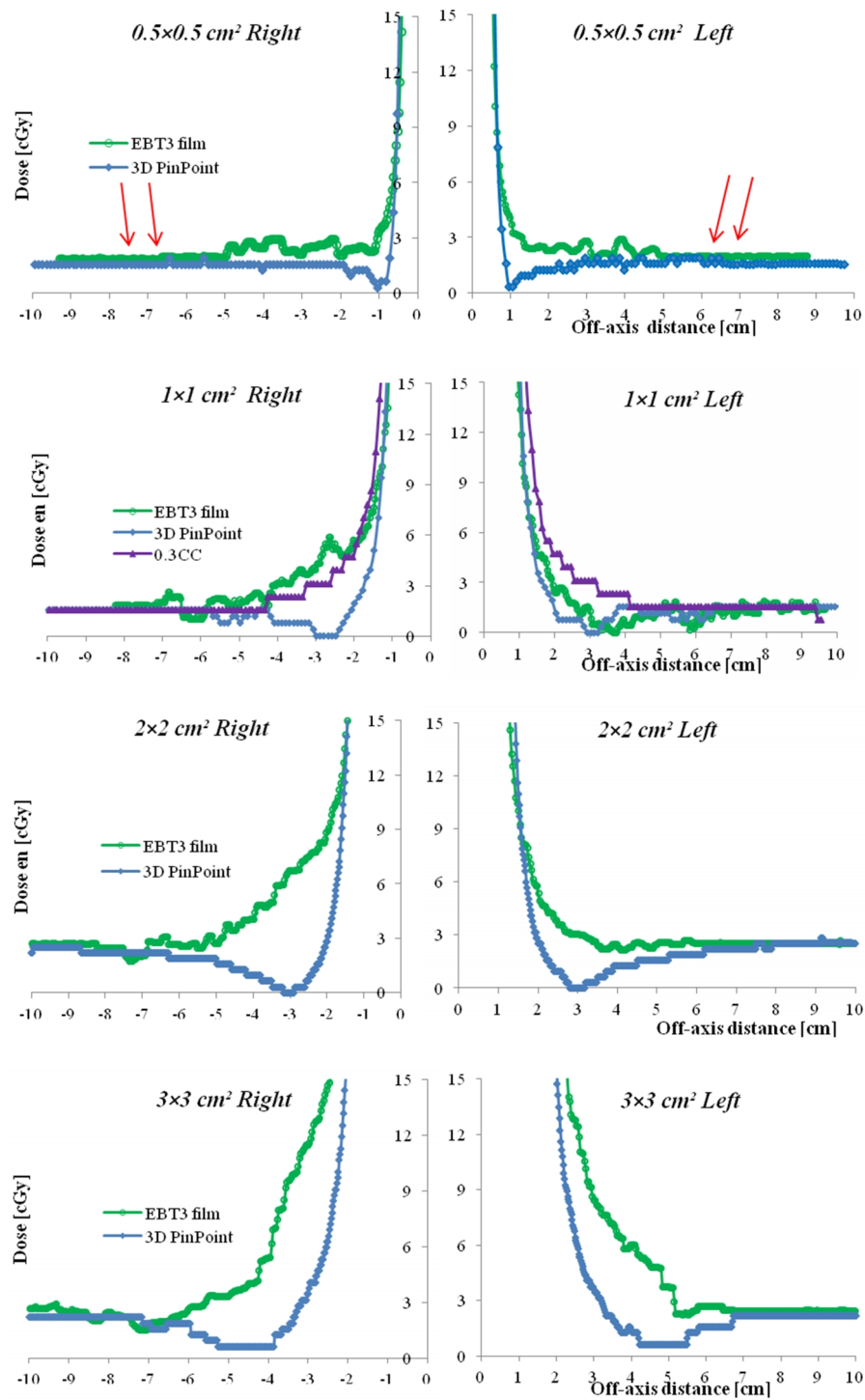


Figure 5: Zoom for profiles for the region outside the field.

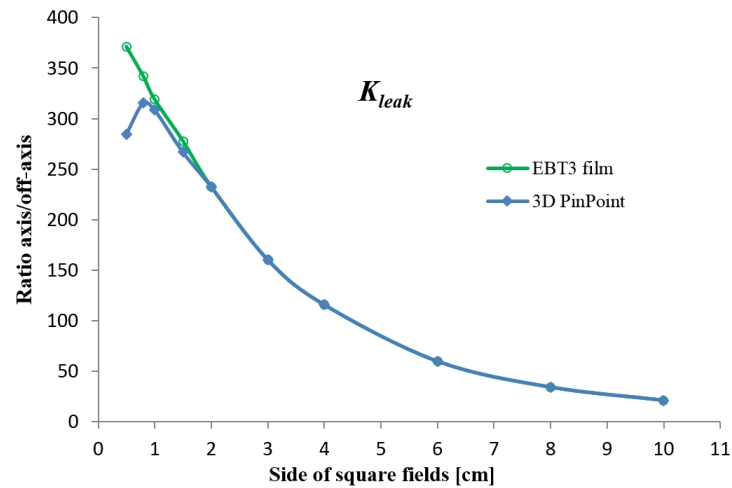


Figure 6: Relationship between K_{leak} and the field size at a 10 cm depth for a 6 MV beam.

Table 3: Comparison between measured and calculated doses using equation 5.

Field size [cm ²] jaws	Measured on-axis dose EBT3 film [cGy]	Measured off-axis dose 3D PinPoint [cGy]	Calculated on-axis dose [cGy]	Diff %
<i>Novalis Tx</i>	<i>400MU</i>			
0.5×0.5	158.4	0.431	160.13	1.09
0.8×0.8	206.13	0.603	204.34	0.87
1×1	221.65	0.695	221.36	0.13
1.5×1.5	244.98	0.877	243.60	0.56
2×2	258.42	1.11	258.69	0.14
0.5×1	208.58	0.606	210.89	1.1
1×2	241.82	0.877	244.08	0.93
1×3	258.46	1.036	260.78	0.89
2×3	265.13	1.33	266.88	0.66
3×2	265.58	1.34	268.88	1.24
<i>TrueBeam</i>	<i>400MU</i>			
0.5×0.5	124.6	0.314	123.04	1.26
0.8×0.8	193.7	0.547	194.48	0.4
1×1	218.3	0.648	215.93	1.09
1.5×1.5	244.53	0.859	243.43	0.45
2×2	254.58	1.047	252.34	0.88
<i>Clinac 600</i>	<i>400MU</i>			
0.5×0.5	145.30	0.387	147.13	1.24
0.8×0.8	198.13	0.575	198.83	0.35
1×1	215.2	0.662	214.90	0.14
1.5×1.5	241.1	0.861	238.65	1.03
2×2	252.66	1.076	250.86	0.72
<i>Novalis Tx</i> MU	Measured on-axis dose EBT3 film [cGy]	Measured off-axis dose at 8 cm by 3D PinPoint [cGy]	Calculated on-axis dose Equation 5	Diff %
0.5×0.5 cm ²				
200	82.26	0.22	81.74	0.63
400	160.5	0.435	161.62	0.69
800	316.88	0.842	312.83	1.29
3×3 cm ²				
200	134.4	0.835	134.6	0.14
400	268.5	1.672	269.4	0.33
800	537.8	3.341	538.4	0.11

4. Discussion

It is noted that the over/under-response of dosimeters are related to sensible volume, density and average atomic number of diode. Moreover, the physical properties and the size of detector are very important characteristic. In this study, the dosimeters showed a significant difference for peak dose and small difference outside the field and in the other hand a compensation factor is needed to avoid the over/under response.

Output factors highly depend on the type of detector. As shown in Figure 3, a wide variation between the 3D PinPoint chamber and the EBT3 films was observed (from 0.4% for the $2 \times 2 \text{ cm}^2$ field to 27.9% for $0.5 \times 0.5 \text{ cm}^2$ field). These results are in agreement with studies in the literature.²³⁻²⁷ In addition, we observed a 2% over-estimation for the $1 \times 1 \text{ cm}^2$ field with the diode according with Underwood *et al.*²³ and Scott *et al.*²⁶ The use of a 3D PinPoint chamber reveals no difference with the EBT3 films from $3 \times 3 \text{ cm}^2$ fields, as shown in Figure 4. However, for smaller fields a signal reduction due to detector in the center of the field was observed with 5.3% and 29.1%, respectively for $1 \times 1 \text{ cm}^2$ and $0.5 \times 0.5 \text{ cm}^2$. We also observed that the effect of the size of the sensitive volume is highly reduced when measuring doses outside the fields.

Calculation of dose from outside of the field coupled with leakage dose has been shown a good agreement with directly measured dose on the central axis. The *A* and *B* parameters in equation (7) depend on the field size, depth and off-axis distance. It has been evaluated using dose measurements with film and chamber for the same condition. Moreover, K_{leak} measurements are not affected by the change of accelerator using 6 MV, as shown in Table 2. The measured dose or that calculated from leakage data would both be suitable for small field sizes. The mean difference between measured and calculated dose values was less than 2% for field size ranging from $3 \times 3 \text{ cm}^2$ to $10 \times 10 \text{ cm}^2$.

5. Conclusion

In this paper, we have developed an analytic model to estimate the on-axis dose in small fields based on the out-of-field leakage measurement. This model can be used to validate dose and output factor measurements.

Conflict of interest

The authors declare that they have no conflicts of interest. The authors alone are responsible for the content and writing of the paper.

References

1. Hassani H, Nedaie HA, Zahmatkesh MH, *et al.* A dosimetric study of small photon fields using

- polymer gel and Gafchromic EBT films. *Med Dosim.* 2014;39(1):102-7.
2. Karl O. Volumetric modulated arc therapy: IMRT in a single gantry arc. *Med Phys.* 2008;35:310.
3. Carmen CP, Ivo AO, WayneB, *et al.* Volumetric Modulated Arc Therapy Improves Dosimetry and Reduces Treatment Time Compared to Conventional Intensity-Modulated Radiotherapy for Locoregional Radiotherapy of Left-Sided Breast Cancer and Internal Mammary Nodes. *J Radiat Oncol Biol Phys.* 2010;76:287-95.
4. Zhu, T. C. Small Field: dosimetry in electron disequilibrium region. *J Phys Conf.* 2010;Ser.250012056.
5. Das IJ, Ding GX, Ahnesjö A. Small fields: non equilibrium radiation dosimetry. *Med Phys.* 2008;35(1):206-15.
6. Bouchard H, Seuntjens J, Duane S, *et al.* Detector dose response in megavoltage small photon beams. *Med Phys.* 2015;42:6033.
7. Bouchard H, Kamio Y, Palmans H, *et al.* Detector dose response in megavoltage small photon beams. II. Pencil beam perturbation effects. *Med Phys.* 2015;42:6048.
8. Wuerfel JU. Dose measurements in small fields. *Medical Physics International.* 2013;8130:04.
9. Wang L, Leszczynski L. Estimation of the focal spot size and shape for a medical linear accelerator by Monte Carlo simulation. *Med Phys.* 2007;34:85.
10. Edwin S, Jan S, Slobodan D, *et al.* Influence of focal spot on characteristics of very small diameter radiosurgical beams. *Med Phys.* 2008;35:3317.
11. Jang SY, Liu HH, Mohan R, *et al.* Variations in energy spectra and water-to-material stopping-power ratios in three-dimensional conformal and intensity-modulated photon fields. *Med Phys.* 2007;34(4):1388-97.
12. Dawson DJ, Schroeder NJ, Hoya JD. Penumbral measurements in water for high-energy x rays. *Med Phys.* 1986;13:101-4.
13. Wolfram U, Wong T. The volume effect of detectors in the dosimetry of small fields used in IMRT. *Med Phys.* 2003;30:341.
14. Le Roy M, De Carlan L, Delaunay F, *et al.* Assessment of small volume ionization chambers as reference dosimeters in high-energy photon beams. *Med Phys.* 2011;56(17):5637-50.
15. Andreo P, Burns D, Hohlfield K, *et al.* Absorbed dose determination in external beam radiotherapy: an international code of practice for dosimetry based on standards of absorbed dose to water. IAEA Technical Report Series No 398 (Vienna: International Atomic Energy Agency). 2006.

16. Almond PR, Biggs PJ, Coursey BM, *et al.* AAPM TG-51 protocol for clinical reference dosimetry of high-energy photon and electron beams. *Med Phys.* 1999;26(9):1847-70.
17. Alfonso R, Andreo P, Capote R, *et al.* A new formalism for reference dosimetry of small and nonstandard fields. *Med Phys.* 2008;35(11):5179-86.
18. IRSN report. Mise au point d'un protocole dosimétrique pour la détermination des FOC dans les mini-faisceaux utilisés en radiothérapie, Report No. PRP-HOM/SDE n°2013-010. 2013.
19. Derreumaux S, Boisserie G, Brunet G, *et al.* Mesure de la dose absorbée dans les faisceaux de photons de très petites dimensions utilisés en radiothérapie stéréotaxique. IRSN Report No. DRPH/SER 2008-18. 2008.
20. Institute of Physics and Engineering in Medicine (IPeM): Small field MV dosimetry. Report No. 103, York, England. 2010.
21. Dutreix A, Bjärngård B E, Bridier A, *et al.* Monitor unit calculation for high energy photon beams. Physics For Clinical Radiotherapy. ESTRO Booklet n°3. 1997.
22. Gafchromic EBT3 white paper. Available from www.gafchromic.com and www.FilmQAPro.com
23. Underwood TSA, Rowland BC, Ferrand R, *et al.* Application of the Exradin W1 scintillator to determine Ediode 60017 and microDiamond 60019 correction factors for relative dosimetry within small MV and FFF fields. *Phys Med Biol.* 2015;(60):6669.
24. Benmakhlouf H, Sempau J, Andreo P. Output correction factors for nine small field detectors in 6 MV radiation therapy photon beams: A PENELOPE Monte Carlo study. *Med Phys.* 2014;41:041711.
25. Bassinet C, Huet C, Derreumaux S, *et al.* Small fields output factors measurements and correction factors determination for several detectors for a CyberKnife and linear accelerators equipped with microMLC and circular cones. *Med Phys.* 2013;40(11):117201.
26. Scott AJ, Kumar S, Nahum AE, *et al.* Characterizing the influence of detector density on dosimeter response in non-equilibrium small photon fields. *Phys Med Biol.* 2012;2157(14):4461-76.
27. Martens C, De Wagter C, De Neve W. The value of the PinPoint ion chamber for characterization of small field segments used in intensity-modulated radiotherapy. *Phys Med Biol.* 2000;45(9):2519-30.